International Conference on

Flow Induced Vibrations

Bowness-on-Windermere, England: 12-14 May, 1987

WAKE FLOW ANALYSIS FOR A HYDROFOIL WITH AND WITHOUT HYDROELASTIC LOCK-IN

Ph. Dupont

and

F. Avellan

Swiss Federal Institute of Technology
Lausanne, Switzerland

M. Wegner

Neyrpic S.A., Grenoble, France

Summary

The influence of the cavitation level on the vortex shedding frequency is used to compare the flow field in the wake of a blunt hydrofoil, with and without hydroelastic lock-in, and with a constant Reynolds number. Accurate LDA measurements allow us to examine in detail the base flow regime considered as the excitation source of the hydroelastic phenomena. Thanks to these measurements a second vortex street superposed on the Karman street has been observed.

Comparisons between measurements and calculations show that a Strouhal number evaluation based on boundary layer displacement thickness agrees well with experiments.

Finally the influence on the configuration of the wake is considered by modifying the shape of the trailing edge.

Held in Bowness-on-Windermere, England. Organised and sponsored by BHRA, The Fluid Engineering Centre. Co-sponsored by the U.K. Atomic Energy Authority Windscale Nuclear Laboratories, the British Nuclear Energy Society and the International Association for Hydraulic Research.

NOMENCLATURE

c	= hydrofoil length	m
d	= vortex line spacing	m
D	= thickness of the truncated trailing-edge	m
$\delta^*_{1\ (2)}$	= displacement thickness on each side of the trailing-edge	m
Δ	= $\Delta' + \delta^*_1 + \delta^*_2$: total displacement thickness	m
Δ'	= separation thickness	m
U_∞	= upstream velocity	ms^{-1}
$U_o(x)$	= velocity of the outer edge of the wake at the x location	ms^{-1}
$\overline{U}(TE)$	= mean value of velocity on both separation loci	ms^{-1}
$\overline{V}_x$, $\overline{V}_y$	= mean velocity components	ms^{-1}
$\overline{v'^2_x}$, $\overline{v'^2_y}$, $\overline{v'_x v'_y}$	= 2nd order moments of velocity fluctuations	m^2s^{-2}
Ω_z	= z component of vorticity vector	m^2s^{-2}
P_∞	= upstream static pressure	Pa
P_v	= vapour pressure	Pa
f_p	= eigen frequency of the hydrofoil	Hz
$\Phi_{xx}(f)$	= power spectrum density for the x component velocity fluctuations	m^2s^{-2}
ρ	= specific mass	$kg \cdot m^{-3}$
ν	= kinematic velocity	m^2s^{-1}
Re	= Reynolds number $Re = U_\infty c/\nu$	-
St	= Strouhal number $St = f \cdot d/U_\infty$	-
S_Δ	= modified Strouhal number $f \cdot \Delta/\overline{U}_{(TE)}$	-
σ	= cavitation number $\sigma = (P_\infty - P_v)/\frac{1}{2}\rho U_\infty^2$	-
T.E.	= trailing edge	

1. INTRODUCTION

Vortex shedding studies are mainly concentrated on the case of the Karman vortex street behind a circular cylinder. About 60 years ago industry began to take an interest in the wakes of plates and profiles in hydraulic machinery (Ref. 1). Several basic investigations were made into wake structure, e.g. (Ref. 2), while research was increased into the problem of the Strouhal number definition, including boundary layer parameters, e.g. (Ref. 3). Because of the increasing specific power of hydraulic machinery, many flow-induced cracks occurred (refs 4, 5 and 6) and safe industrial solutions were demanded as a result of geometrical modifications of the trailing edges (Ref. 7). Knowledge of the excitation structure was improving, but the obstacle of the interaction between the excitation process and mechanical response had to be faced, including the resulting noise (Ref. 8). The influence of cavitation also began to be taken into account (Ref. 9).

This contribution attempts firstly to clarify the wake structure of a truncated NACA 009 profile when there is hydroelastic behaviour. Both the mean and unsteady velocity values were obtained by two-component L.D.A. measurements in the wake of a truncated hydrofoil, and were compared to acoustic measurement in the vicinity of the hydrofoil. One original aspect of this is that lock-in or lock-off between flow and mechanical structure are not obtained by a change in velocity, but by a change in cavitation number. The influence of the degree of cavitation on wake frequencies is therefore checked and confirmed. An analysis of these results makes it possible, on the one hand, to understand better the velocity field in the wake and, on the other hand, to check the Strouhal number obtained with boundary layer displacement thickness. Finally, some information is given on the influence of trailing-edge geometry.

2. EXPERIMENTAL SET-UP

The experiments were done in the cavitation water tunnel at the Institut de Machines Hydrauliques et de Mécanique des Fluides of the Swiss Federal Institute of Technology, Lausanne.

Three kinds of measurements were taken. Firstly, visualisations using a classic strobe flash. Secondly, acoustic measurements using a hydrophone (BK 8103) installed in a vessel (see Fig. 1). The BK 8103 amplifier output signal was analysed by an FFT HP 3582A spectrum analyser. Thirdly, the flow field was investigated by a two-component laser-Doppler anemometer (DANTEC 55X). The LDA output data were processed and stored on a DEC LSI 11/73.

A 100 mm-wide 2-D NACA 009 profile, truncated to 90% and with a 3.6 mm-thick trailing edge was maintained at zero incidence. The hydrofoil was fixed on one side and supported by a 10 mm rod on the other side. The first ten elastic modes were calculated, with a finite element software developed by Neyrpic S.A. The main calculations are summarised in Table 1, and the hydrofoil deformation pictures are shown in Fig. 2 for the first three vibration modes.

3. EXPERIMENTAL RESULTS

3.1. Visualisations

The spatial arrangement of the shedded vortices was made apparent by cavitation of the vortices' core centre. Without lock-in the vortex arrangement shows a 3-D behaviour corresponding to the excited mode of the hydrofoil, see Fig. 3a. In the lock-in flow conditions, the second mode, i.e. the torsional mode, induced a 2-D arrangement of these shedded vortices (fig. 3b). Surprisingly, if the pressure value was decreased the frequency lock-in phenomenon was eliminated, and the vortex street cavitation then disappeared.

3.2. Velocity Measurements

The following L.D.A. measurements were made with a constant upstream velocity and at two different static pressure levels, corresponding to a σ value of 1.47, frequency lock-in case, and to a σ value of 0.67 respectively without lock-in. Five mean velocity transverse profiles were measured in the wake of the hydrofoil. The results for these two cases are shown in Fig. 4. Typical RMS and mean values of the velocity are shown in Fig. 5 by a transverse section at the locations of x = 3.5 mm and 5.0 mm behind the trailing edge. Spectral analysis by Fourier transform of the velocity correlation function gave the power spectrum density function. Typical results are shown in Fig. 6 for the two cases at the x = 5 mm location.

3.3. Acoustic Measurements

Acoustic measurements were taken for the whole range of velocities from 5 m/s to 35 m/s and various static pressure levels. In Fig. 7 three noise power spectra are superposed, showing the influence of the σ value by keeping the upstream velocity constant (U_∞ = 12.75 m/s). The frequency lock-in conditions were verified from σ = 4.1 (no cavitation) to σ = 1.47 (moderate cavitation). Acoustic evidence of the frequency lock-in phenomenon is shown in Fig. 10. Moreover, to show the trailing-edge geometry effects, three acoustic spectra are shwon in Fig. 8 corresponding to the actual geometry, and to a 45^0 trailing-edge and 25^0 trailing-edge. In these measurements the flow was free of cavitation at 24.7 m/s. It was noted that the second mode of vibration (torsional) induces a 35 dB acoustic amplification for lock-in conditions with the actual trailing-edge. Meanwhile, bending mode 1 induces a 20 dB acoustic amplification with the 25^0 trailing-edge and for U_∞ = 6 m/s.

4. ANALYSIS

4.1. Base Flow Analysis

The strong influence of the cavitation number on the vortex shedding frequency (see Fig. 9) gave us the opportunity to study the base flow, considered as the excitation source of the hydroelastic phenomenon, by keeping the Reynolds number constant. The excellent quality of the L.D.A. velocity measurements allowed us to obtain stream lines and vorticity fields for the base flow and for the wake of the hydrofoil without lock-in (see Fig. 11). In this figure high vorticity regions and recirculating flow are readily shown and correspond to the path of the shedded vortices, limiting the base flow region where there is a pair of fixed vortices.

In the velocity vector profiles (Fig. 4a), Karman vortex trajectories are also fairly apparent. In the same figure, in the lock-in case, a second high vorticity region appears. In this case the base flow fluctuates so much that it prevents us from seeing the previous pair of fixed vortices. Using the vortex line spacing d measured on photographs (Fig. 3) and the Karman frequency f_K in Fig. 6, we can determine the convective velocity U_K of the vortices by the relation $U_K = f_K \cdot d$. Taking this value on the mean velocity profile at a given location, we can determine the y coordinate of the Karman street (see Fig. 5). However, RMS distribution at the same location reaches a local maximum (Fig. 5). If we associate this RMS distribution behaviour with the presence of a vortex path, another local maximum can be seen, which suggests the existence of a second vortex street, both on the x = 3.5 mm and x = 5 mm velocity profiles. Moreover, the location of this hypothetical street corresponds to the above-mentioned high vorticity region. The existence of a second vortex street can be confirmed by the amplification of the second harmonic on the power spectrum (Fig. 6). Hence, convective velocity U_{K2} associated with the second street is half the previous convective velocity U_{K1}, as shown in Fig. 5. Nevertheless, definite proof of the existence of a second vortex street in the base region with lock-in could be obtained using spatial correlation techniques.

4.2. Strouhal Number Evaluation

The displacement thickness Δ and the outer mean velocity $\bar{U}$ at the trailing edge were used to calculate the Strouhal number S_Δ. A first application for the truncated TE can be given by $\sigma = 0.67$ and $U_\infty = 12.75$ m/s, i.e. without lock-in effect (central frequency = 960 Hz) (see Table 2). The Strouhal number based on L.D.A. measurement therefore has an intermediate value between both calculations based on the displacement boundary layer. If acoustic measurements are now considered for the whole non-cavitating and non-interacting operating range, e.g. 15 m/s$<U_\infty<$35 m/s, S_Δ values based on the measured frequency and calculated wake thickness values remain between 0.255 and 0.265. Concerning other TE equipped with 45^0 and 25^0 edges, although the excitation peaks are less organized, the same calculation procedure leads to S_Δ values of between 0.250 and 0.270. It therefore seems convenient to base a reasonable prognosis on those S_Δ values for non-cavitating flows. When cavitation begins, the Strouhal number may be increased by about 15%.

4.3. Trailing-Edge Geometry Influence

Although L.D.A. measurements were not taken when the TE shape was changing, significant conclusions can be drawn from the acoustic measurements. Without lock-in, e.g. $U_\infty = 24.7$ m/s the blunt trailing edge shows that an acoustic spectrum rather different from those of the TE with 45^0 and 25^0 edges (Fig. 8). The truncated TE leads to a well-formed peak around 1,500 Hz, which corresponds to a Strouhal number $S_\Delta = 0.26$.

The TE with shaped edges does not present a typical peak, but a rather wide amplification range around 2,500 Hz if compared to the basic noise. Again, the central frequency corresponds to $S_\Delta = 0.26$ and we checked that linear Strouhal law agrees up to 40 m/s. There is a lock-in range for the TE with shaped edges as well, for the same 820 Hz mode, but for a lower velocity $\sim$ 7 m/s. The relevant Strouhal number $S_\Delta = 0.26$ remains quasi constant. For the very low velocity range, e.g. $U_\infty<5$ m/s, it seems that organization in the spectrum of the truncated TE disappears, while typical peaks arise in the spectra with edges. This rather paradoxical result must be confirmed by L.D.A. measurement. If confirmed it could be concluded that for a relatively well formed TE, wake organization could be stronger at a low Reynolds number than for a higher one, therefore conflicting with other references (Ref. 10).

5. CONCLUSIONS

Accurate and detailed L.D.A. measurements allowed us to analyse the base flow region of a hydrofoil's blunt trailing edge. Influence of the cavitation number on the shedded vortices' frequency is clearly shown. This particularity was used to compare two flows corresponding to situations with and without lock-in by keeping the Reynolds number constant. It was clearly shown that, in the lock-in situation, a second vortex street was created in the base flow region with a convective velocity half that of the external Karman vortices.

Acoustic frequencies obtained by noise measurement were confirmed by the L.D.A. measurements in both situations, with and without cavitation.

Both experimental and theoretical values of the boundary layer thickness confirm very well the Strouhal number predicted by previous anthors. This good agreement was also found for the sheped trailing edge.

Systematic acoustic study, using a wide range of Reynolds numbers, of three different trailing-edges shows that sheped trailing edges have a less organized structure than blunt ones for a high Reynolds number. However, at a low Reynolds number $Re = 5 \cdot 10^5$, the shaped trailing-edge wake seems to have an organized configuration. This particularity can be of a certain importance in model testing.

6. ACKNOWLEDGEMENTS

The authors would like to thank Professor I.L. Ryhming for his comments and suggestions and Mr. Vuillerod, of Neyrpic, who calculated the eigen frequency by the finite element method. This research was made possible by financial support from the Swiss "Commission d'Encouragement à la Recherche Scientifique" (CERS) and the Swiss "Nationaler Energie Forschungs Fonds" (NEFF).

7. REFERENCES

1. Heskestad, G. and Olberts, D.R.: "Influence of trailing edge geometry on hydraulic turbine blade vibrations resulting from vortex excitation", ASME, Paper 59, Hyd. 7.
2. Blake, W.K.: "A statistical description of pressure and velocity fields at the trailing edges of a flat strut", D.W. Taylor naval ship research and development center, Report 4241, 1975.
3. Griffin, O.M.: "A universal Strouhal number for the 'locking-on' of vortex shedding to the vibrations of bluff cylinders", J. Fluid Mech., vol. 85, 1978, part 3, pp. 591-606.
4. Grein, H. and Staehle, M.: "Rupture par fatigue d'entretoises d'avant-distributeurs de grandes turbines", Bulletin Escher Wyss, No. 1, 1978.
5. Ulith, P.: "Flow induced cracks on stay vanes", Symposium IAHR/IUTAM, Karlsruhe, 1979.
6. Casacci, S., Lourdeaux, B. and Wegner, M.: "Dynamic behaviour of large Francis stay-rings", IAHR Symposium, Amsterdam, 1982.
7. Heinemann, H.J. and Bütefisch, K.A.: "Determination of the vortex shedding frequency of cascades with different trailing edge thicknesses", AGARD-CP-227, 1977, pp. 35-1-35-11.
8. Naudascher, E. and Rockwell, D.: "Oscillator model approach of flow induced vibrations in a system", J. of Hydraulic Research, vol. 18, No. 1, 1980.
9. Rao, B.C.S. and Petrikat, K.: "The vortex induced vibrations of a flat plate in cavitating flow", IAHR Symp., Colorado, 1978, vol. II.
10. Blake, W.K.: "Excitation of plates and hydrofoils by trailing edge flows", J. of Vibration, Acoustics, Stress in Design, July 1984, vol. 106.

TABLE 1

Mode		1st	2nd	3rd
Calculated f_p in air	(Hz)	1062	1062	3228
Measured f_p in air	(Hz)	1100	1020	3500
Measured f_p in water	(Hz)	610 - 630	820 - 880	2220-2280
Calculated f_p water/f_p air	(-)	0.547	0.729	0.547
Measured f_p water/f_p air	(-)	0.55 - 0.57	0.80 - 0.86	0.63-0.65

TABLE 2

Imput data	$\delta_1^* = \delta_2^*$	$\bar{U}_{(TE)}$	Δ	$f \cdot \Delta / \bar{U}_{(TE)}$
Theoretical calculation (Truckenbrodt, Head)	0.26 mm 0.40 mm	14.03 m/s	4.12 mm 4.40 mm	0.282 0.301
L.D.A. measurements	-	13.40 m/s	4.40 mm	0.287

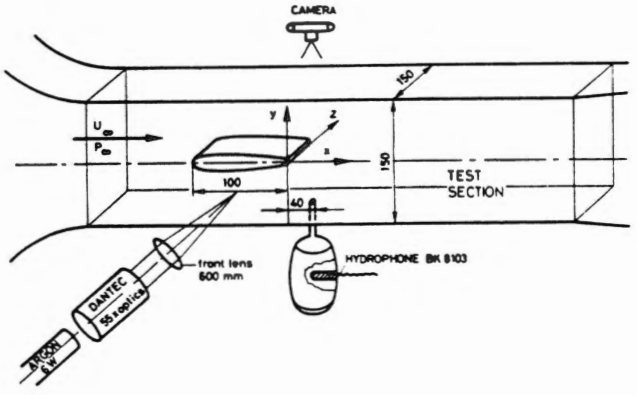

Figure 1: Diagram of experimental set-up

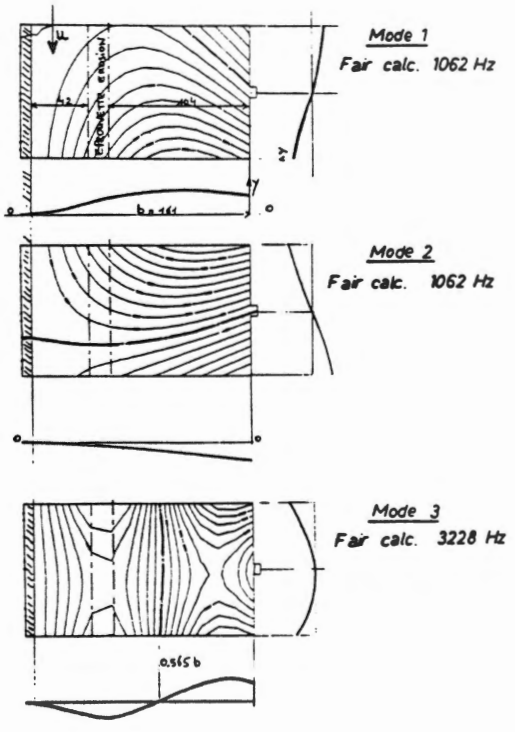

Figure 2: Three first vibration modes (finite elements calculation)

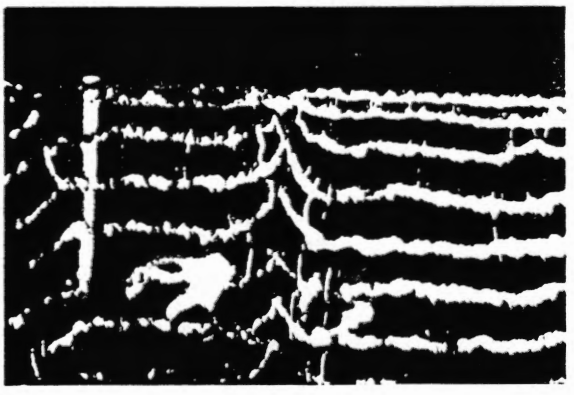

a.

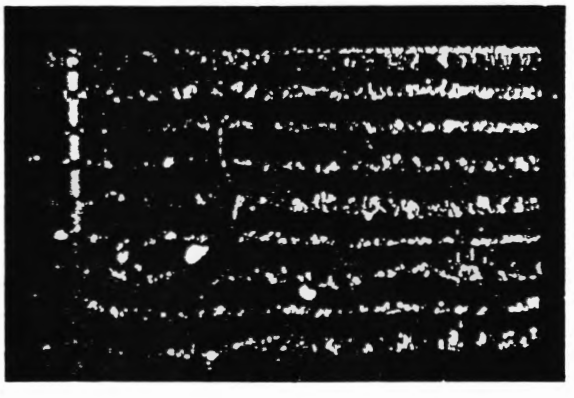

b.

Figure 3: Karman vortex cavitation (a. without lock-in and b. with lock-in)

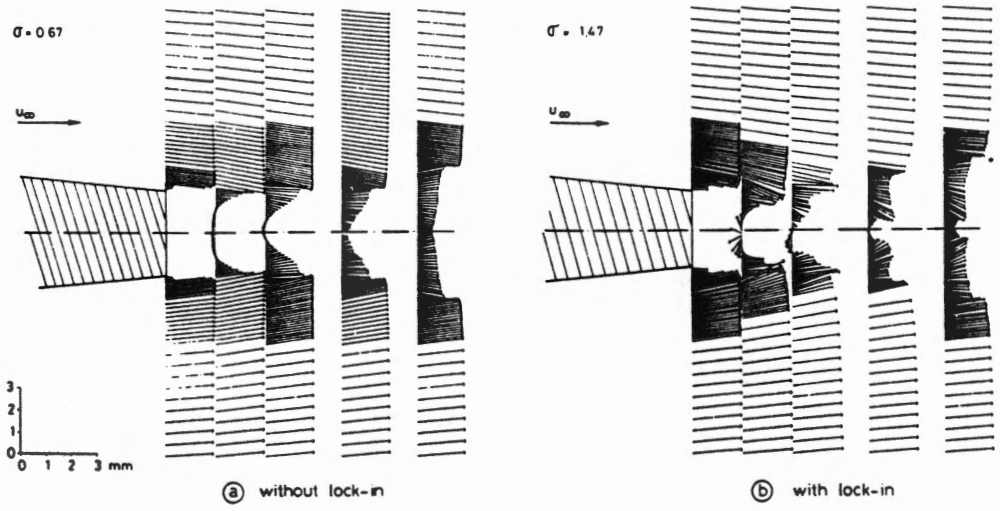

Figure 4: Vectorial mean velocity (2-D) in the wake of the hydrofoil

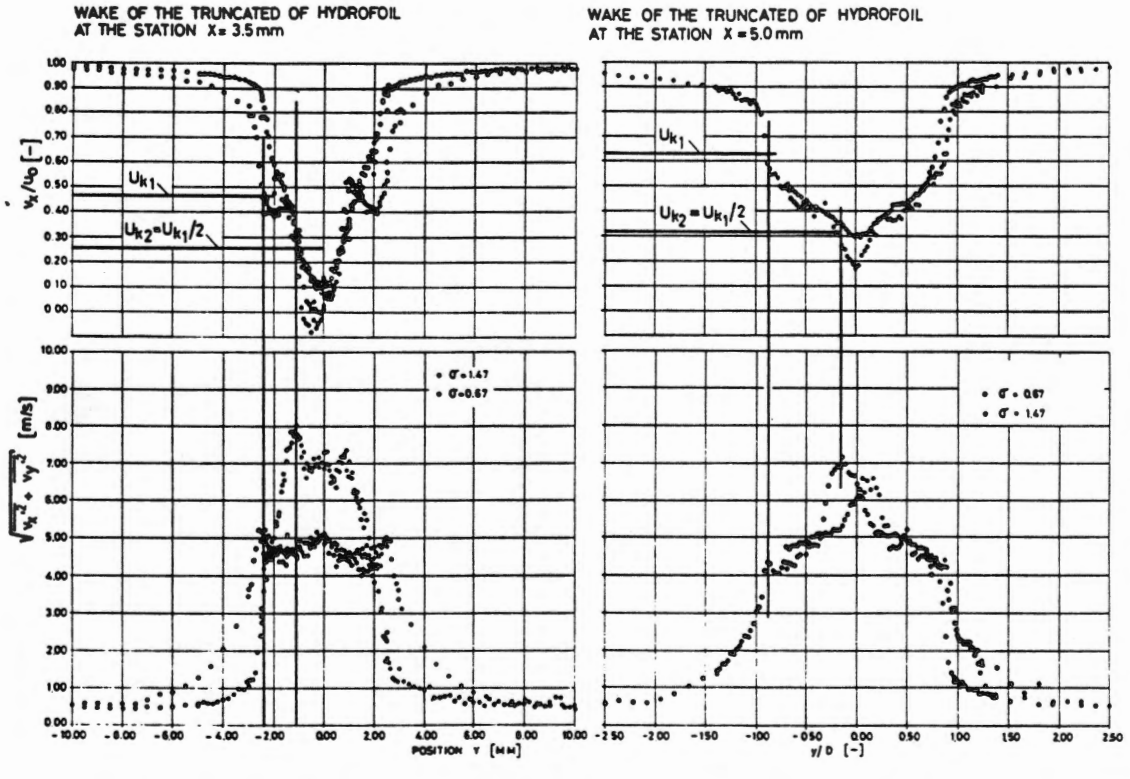

Figure 5: Mean velocity and RMS value transverse profiles at two stations*

**Note that for the x = 3.5 mm station the y coordinate is not normalized by the thickness D.*

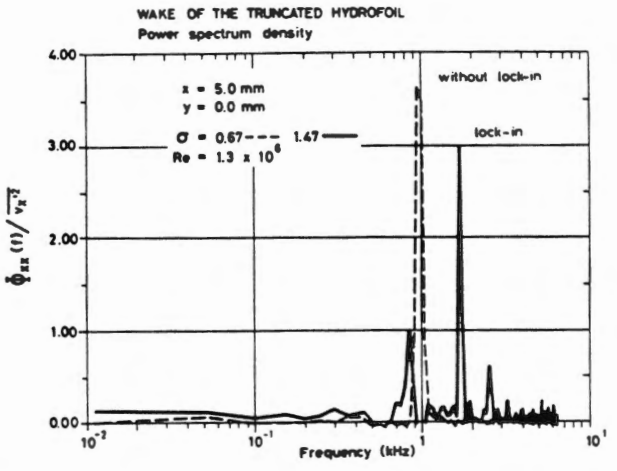

Figure 6: Fourier analysis of velocity fluctuations with and without lock-in

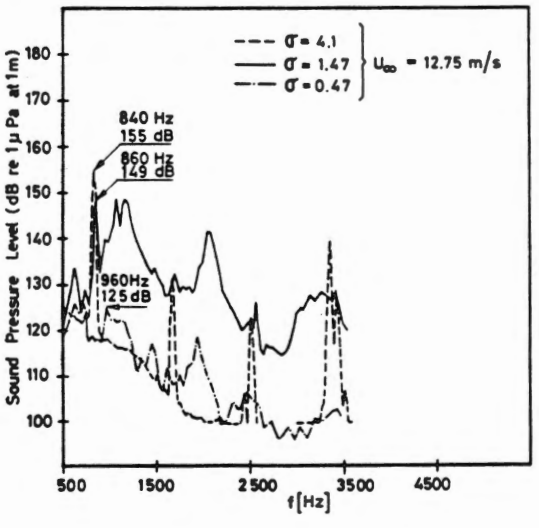

Figure 7: Cavitation influence on noise power spectrum

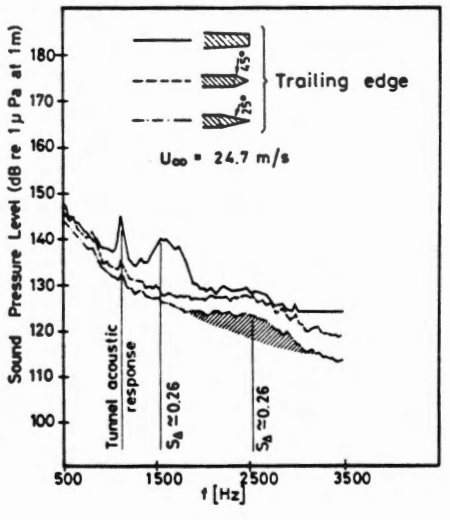

Figure 8: Trailing edge geometry influence on noise power spectrum

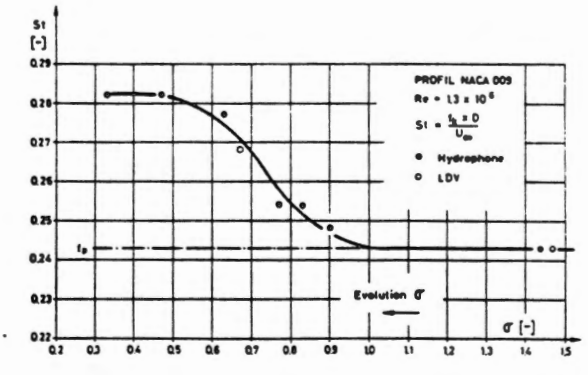

Figure 9: Cavitation influence on lock-in phenomenon

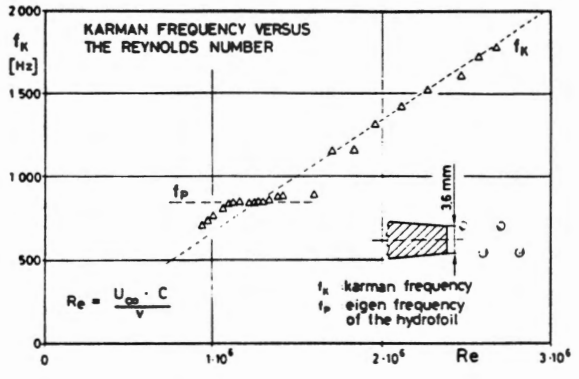

Figure 10: Influence of lock-in on Karman frequency (acoustic measurements)

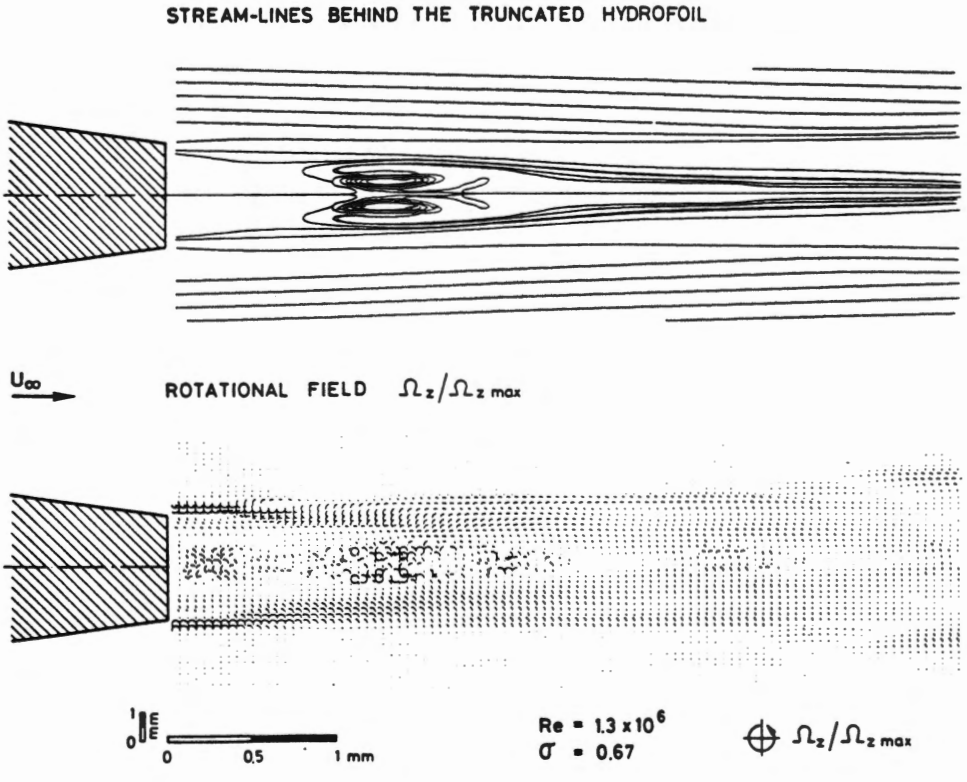

Figure 11: Flow field without lock-in (based on L.D.A. measurements)